

PSFC/JA-00-8

Simultaneous Soft X-Ray Emissivity Profile Measurements

in Delaigle, S. et al. (eds) Proceedings of the 1999 International Conference on X-Ray Spectroscopy, Vol. 1, pp. 1-10



Provided by DSpace@MIT

[Metadata, citation and similar papers at core.a](#)

T. Sunn Pedersen, R.S. Granetz

March 2000

Plasma Science and Fusion Center
Massachusetts Institute of Technology
Cambridge, MA 02139 USA

This work was supported by the U.S. Department of Energy, Cooperative Grant No. DE-FC02-99ER54512. Reproduction, translation, publication, use and disposal, in whole or in part, by or for the United States government is permitted.

Submitted for publication to *Review of Scientific Instruments*.

Simultaneous soft x-ray emissivity profile measurements in poloidally separate locations of the Alcator C-Mod edge plasma

T. Sunn Pedersen and R. S. Granetz

MIT PSFC, Cambridge, MA 02139, USA

Two high resolution edge x-ray imaging diagnostics have been installed in the Alcator C-Mod tokamak. One array measures the radial soft x-ray emissivity profiles at the top of the plasma with 1.2 mm radial resolution, mapped along flux surfaces to the midplane, whereas the other measures the radial soft x-ray emissivity profiles at the outboard edge with 1.5 mm radial resolution mapped to the midplane. The two diagnostics measure the chord brightness profiles, which are then inverted to get soft x-ray emissivity simultaneously with a 12 μ s sampling time. This allows us to determine if the soft x-ray emissivity, and therefore the fluorine density, is constant on a flux surface during steady state high confinement mode conditions, as well as during fast transient edge events, such as Edge Localized Modes or transitions from the high confinement mode to the low confinement mode. Measurements are presented showing that the soft x-ray emissivity is not constant on a flux surface, but instead

shows a large poloidal variation, contrary to what is assumed in the inversion routine. The effects of the poloidal variation on the inversion accuracy are estimated numerically. It is found that the emissivity is systematically overestimated at the top, and underestimated at the outboard edge, by less than 15%. The width of the x-ray emissivity pedestal is accurate to within 15%, and the location of the pedestal is accurate to within 1 mm. Measurements showing a poloidal propagation delay for the onset of the transition from high confinement mode (H-mode) to low confinement mode (L-mode) are also presented.

I. Introduction

In tokamak plasma fusion experiments the confinement of particles and energy is much lower than what is expected from neoclassical theory. This enhanced transport, which is believed to be due to microturbulence, is usually observed across the whole plasma profile. However, with sufficient heating power, it is possible to trigger a transition from this low confinement mode (L-mode) to a high confinement mode (H-mode).¹ There is a significant improvement in the global confinement times of particles and energy, even though the large change in transport coefficients occurs only locally in a narrow layer near the plasma edge. This layer is referred to as the edge transport barrier, or the pedestal region, since the local improvement of confinement leads to steep edge gradients and pedestal-like shapes for the radial profiles of various plasma parameters such as electron density, electron temperature, and soft x-ray emissivity. Because of the improvement in confinement, the H-mode transport barrier has been studied extensively on tokamak experiments. On Alcator C-Mod, which is a high magnetic field, high plasma density, shaped tokamak, the H-mode barrier is particularly narrow, with typical scale lengths on the order of 2-8 mm. This paper describes an edge soft x-ray imaging system which simultaneously measures the soft x-ray emission from the edge transport barrier region in two poloidally separate locations. In a previous publication, measurements of soft x-ray emissivity, electron density and electron temperature profiles at the outboard edge were used to derive detailed information about the radial transport of fluorine in the transport barrier region.² Having two poloidally separate simultaneous measurements of the soft x-ray emissivity rather than just one allows us to determine if the soft x-ray emissivity shows any strong poloidal variation, both in steady state conditions and during transient edge events such as Edge Localized Modes (ELMs),³ and H-mode to L-mode transitions. The x-ray emissivity profiles are derived from the brightness profiles by assuming

that the emissivity is constant on a flux surface. We show that the x-ray emissivity is far from constant on a flux surface near the H-mode edge, and investigate the consequences for the accuracy of the inversion. We also present measurements of the x-ray emissivity profiles at the H-mode to L-mode transition, showing that the flattening of the pedestal begins at the outboard edge before it begins at the top of the plasma.

II. Description of the two arrays

The views of the two soft x-ray arrays in the Alcator C-Mod vessel are shown in Figure 1. One array views the edge plasma at the top, whereas the other array views the outboard edge just above the midplane. Each array consists of 38 photodiodes viewing the plasma through a narrow slit aperture, which is 0.5 mm in the poloidal direction and 36 mm in the toroidal direction. Behind each aperture is a 10 μm beryllium foil which acts as a photon filter, cutting out photons with energies below 500 eV and having 50% transmission at 1150 eV photon energy. Soft x-ray brightness profiles are obtained for each photodiode array, representing essentially the integrals of the local x-ray emissivity along the lines of sights of the detectors. For the purpose of inverting the chord integrated measurements into a local emissivity profile, we assume that the x-ray emissivity is a flux function, as given by the magnetic reconstructions. This allows us to solve for the x-ray emissivity as a function of the flux coordinate by matrix inversion, using singular value decomposition. As will be discussed in this paper, this assumption is not valid at the plasma edge, but the emissivity profiles are still relatively accurate. Details of the filter function, the photodiodes, and the singular value decomposition method are the same as those from the previous single-array soft x-ray edge diagnostic, and can be found in Reference 4. For convenience, we always plot the soft x-ray emissivity as a function of the major radial coordinate, rather than as a

function of the flux coordinate. The two are uniquely related as follows. For a given flux surface, the equivalent major radius is defined as the major radius of this flux surface at the outboard midplane of the plasma. Because of the flux expansion, we get a better midplane radial resolution at the top of the plasma (1.2 mm mapped to the midplane) than at the outboard edge (1.5 mm mapped to the midplane), even though the real chord spacing is 2 mm at the top and about 1 mm at the outboard edge. The radial resolution of the emissivity profiles can be improved to 0.8 mm for the top array and 1.0 mm for the outboard edge array, but due to the increased noise sensitivity, such a high radial resolution is not routinely used in the matrix inversions. The sampling time can be varied from 12 μ s (83 kHz) to 200 μ s (5 kHz), but the response time of the electronic amplification is 30 μ s in the present setup, thus smoothing out the response to very fast transients measured at the highest sampling rates. By having two poloidally separate views of the same flux surfaces, with identical beryllium filters and photodiodes, we can measure if the soft x-ray emissivity varies along a flux surface between the outboard edge and the top of the plasma. In order to make such comparisons accurately, it is necessary to know the absolute position of each of the detector views, and the areas of the apertures. The positions of viewing chords have been determined with 1-2 mm uncertainty at the vessel walls for both arrays. This corresponds to less than 1 mm uncertainty mapped to the midplane. The difference in aperture areas between the two arrays is less than 5%. This was established by shining a uniform source of brightness through each of the apertures (without the beryllium foils) onto the same photodiode array. The difference in photodiode signal between the two apertures was less than 3%.

III. Steady state H-mode results

X-ray emissivity profiles at the top and the outboard edge just above the midplane have been obtained for a wide variety of plasma discharges. The measurements at the outboard edge just above the midplane are very similar to the measurements which were made at the outboard edge just below the midplane with the previous single array edge x-ray diagnostic.⁴ Soft x-ray emissivity levels at the edge are low in L-mode, on the order of $0.5\text{-}3\text{ kW/m}^3$, and the emissivity profile usually does not have a pedestal-like shape. In H-mode, the emissivity profile at the outboard edge becomes distinctly pedestal-like, with emissivity levels typically in the range from $10\text{-}50\text{ kW/m}^3$ at the top of the pedestal, ie. much higher than in L-mode. The pedestal width at the outboard edge can vary from $1.5\text{-}8\text{ mm}^2$,⁴ smallest in Edge Localized Mode (ELM) -free H-modes, and largest in type III ELMy³ H-modes, and EDA H-modes.⁵ The edge x-ray emissivity profile measured at the top of the plasma also becomes pedestal-like in H-mode, but the pedestal is always located closer to the nominal separatrix, usually within 2 mm. The pedestal height at the top of the plasma is usually smaller than at the outboard edge, and the pedestal width at the top is typically 1.5-3 mm. The largest differences in pedestal parameters are observed during low current (high q_{95}) EDA H-modes, where the difference in pedestal position (mapped to the midplane) is on the order of 12 mm, and the difference in pedestal width usually exceeds a factor of 2, with the pedestals being wider at the outboard edge. A comparison between the edge radial emissivity profiles at the top and the outboard edge is shown in Figure 2 for such a high q_{95} EDA H-mode. The most apparent difference is perhaps in pedestal location. At the top of the plasma, the x-ray pedestal is just inside the separatrix (2 mm inside) whereas it is well inside the separatrix at the outboard edge (13.7 mm inside). The pedestal is 5.0 mm wide at the outboard edge but only 1.8 mm at the top of the plasma. The height is about 20 kW/m^3 at the outboard

edge and 14 kW/m^3 at the top of the plasma. The slopes inside the pedestals are roughly in agreement (0.91 MW/m^4 at the outboard edge and 1.0 MW/m^4 at the top).

IV. Implications for the inversion accuracy

The uncertainties in the EFIT reconstruction of the flux surfaces are too small to account for the differences in the pedestal characteristics between the outboard edge and the top of the plasma. There are real asymmetries in the soft x-ray emissivity, indicative of a strong poloidal variation in the impurity (fluorine) density near the separatrix. This issue will be addressed in detail in a future publication. Here, we concern ourselves with the implications for the accuracy of the inversion from chord integrated emissivity to local emissivity. As mentioned, the inversion is made under the assumption that the x-ray emissivity is constant on a flux surface, as given by the EFIT reconstruction. X-ray emissivity profiles derived from measurements using this assumption directly contradict the assumption. The inversion accuracy is therefore affected, and the magnitude of the error depends on the extent to which the contours of constant emissivity deviate from the EFIT flux contours. It does not depend on the degree to which this deviation is caused by real poloidal variations of x-ray emissivity on a flux surface, or caused by a discrepancy between the real flux surfaces and EFIT flux surfaces. Fortunately, each detector array views only a small poloidal cross section of the plasma, so even if the soft x-ray emissivity contours deviate significantly from the EFIT flux contours, the deviation in the view of each array might still be small.

In order to perform the inversion accurately we must know the shape of the emissivity contours, but this shape can only be accurately measured if we perform two-dimensional tomography at the plasma edge. With the present detector views, this is not possible. However, we can still *estimate* the magnitude of the inversion error introduced via the erroneous

assumption that the EFIT flux contours also are the contours of constant emissivity. The following method is used:

- We prescribe a certain two-dimensional x-ray emissivity function whose contours do not follow the contours of constant flux Ψ . The deviation is chosen to fit the experimental data, that is, we use a narrow pedestal shape for the x-ray emissivity near the separatrix but place the pedestal right at the separatrix at the top of the plasma and about 10 mm inside the separatrix at the outboard midplane.
- We then calculate the signal on each detector by integrating the emissivity function along the line of sight of the detector. The resulting brightness profiles should look similar to measured brightness profiles.
- These brightness profiles are inverted using the standard algorithm, that is, under the assumption that the emissivity *is* constant on a magnetic flux surface.
- The resulting emissivity profiles for the two arrays will be different from each other, as they should be, given that the local emissivity is different in the two views. We can compare the emissivity obtained from the outboard edge array with the prescribed two-dimensional emissivity function in its field of view. Similarly, we can compare the prescribed two-dimensional emissivity function at the top of the plasma with the emissivity deduced from the top array.
- This will give us a measure of how well the arrays measure the *local* emissivity in their fields of views.

The inversion error will depend on the particular choice of the two-dimensional emissivity function, so several different shapes have been used. Figure 3 shows a particular choice of

a two-dimensional emissivity function. The emissivity contours deviate significantly from the EFIT flux contours, in particular at the top of the plasma. The emissivity has been chosen to have a pedestal-like shape at the edge of the plasma, and the pedestal is near the separatrix at the top of the plasma, but about 10 mm inside it at the plasma midplane, in agreement with typical measurements. Integrating this emissivity function along the line of sight of each detector, we find brightness profiles for both arrays which closely resemble brightness profiles obtained from real plasma measurements. These brightness profiles are then used as inputs into the standard inversion routine, which (erroneously) uses the EFIT flux contours as the contours of constant emissivity. The resulting emissivity profiles are shown in Figure 4. The pedestal derived from the outboard array is located about 10 mm further inside the separatrix than that derived from the top array, similar to what is observed in real experiments. This gives us confidence that the prescribed emissivity contours deviate from the flux contours by about the right amount. In the real data, the pedestal is usually wider at the midplane, whereas it is slightly wider at the top in the simulated data used here.

We now estimate the extent to which the emissivity profile derived from the array viewing the outboard edge accurately matches the prescribed emissivity profile in its field of view. We can choose to compare anywhere in the field of view of the array, but the best match is roughly in the center of the view. Such a comparison can be seen on Figure 5. Similarly, on Figure 6 we compare the emissivity at the top of the plasma with that derived by the array viewing the top of the plasma. In both cases, the width and position of the local pedestal are accurately reproduced — the width is accurate to 2% at the outboard midplane and 9% at the top of the plasma, and the pedestal positions are within 1 mm of the pedestal position of the prescribed emissivity. The emissivity derived from the outboard array overestimates the prescribed emissivity by about 5%, whereas the emissivity derived from the top array

underestimates the prescribed emissivity by about 10%. The outboard array produces more accurate results because the emissivity contours follow the flux contours rather well at the outboard midplane but deviate more strongly from them at the top. The fact that the top array underestimates the emissivity, and the outboard midplane array overestimates it, can be understood qualitatively. A detector in the top array measures essentially the integral of the emissivity along the line of sight of the detector. At the top of the plasma, the emissivity contours have a smaller radius of curvature than the flux contours, so when we assume that the emissivity is constant on a flux surface, we are overestimating the radius of curvature, and thus the path length of the integral. This will lead to an estimate of the emissivity which is too low. At the outboard edge, the radius of curvature is underestimated, leading to an estimate of the emissivity which is too high.

Several other examples of emissivity contours have been tried. As expected, the accuracy of the inversion is determined for each array by the extent to which the emissivity contours deviate from the flux contours within the view of the array, so depending on the exact choice of emissivity shape, the largest inversion errors may occur for either array. For the various emissivity functions studied here, we find that the emissivity profiles derived from both arrays are in good agreement with the local emissivity in the views of the detectors. There is a systematic but small (less than 15%) overestimation of the emissivity at the outboard edge and a similar underestimation at the top of the plasma. In cases where the inversion error is large (close to 15%) at the outboard edge, it is small at the top, and vice versa. The pedestal widths are accurate to within 15% as well. This error is smaller than the typical uncertainty in the width introduced by random noise, which is on the order of 20%. The position of the pedestal is accurately determined to within 1 mm. We therefore find that the inversion errors are small enough that they do not significantly affect our ability to make detailed comparisons between the emissivity profiles at the outboard edge and the top of the

plasma.

V. Measurements of transient phenomena

Having two *simultaneous* measurements of the soft x-ray emissivity allows us to study the temporal evolution of fast events such as ELMs or H-L transitions to see if such transient events occur simultaneously in the two different poloidal locations, or if there is a timing difference large enough to be detectable. In a few cases, we have been able to establish that the onset of the flattening of the x-ray emissivity pedestal, presumably indicative of the large change in confinement at the H-L transition, occurs at the outboard edge before it occurs at the top. The observed timing differences are on the order of 10-20 μs . Timing differences down to 12 μs can be detected, even though the electronic amplification circuit has a 30 μs RC time constant, if the signal perturbation in question is rather large. Since the x-ray pedestal is completely destroyed in about 100 μs after the H-L transition, the change in soft x-ray signal from time sample to time sample can be large, particularly in cases where the emissivity was large before the transition. An example of a timing difference in the x-ray pedestal flattening is presented in Figure 7, where we show the emissivity profiles at 4 consecutive time samples, two immediately before and two immediately after the pedestal starts flattening at the outboard edge. The onset of the pedestal collapse is delayed by at least one, and possibly two time samples at the top of the plasma compared to the outboard edge.

A. Implications of the timing difference at the H-L transition

The timing difference observed between the outboard edge and the top of the plasma implies that the instability that destroys the H-mode transport barrier is a mode which causes large radial transport at the outboard edge before it affects the radial transport at the top of the plasma. A likely explanation is that the mode is of a ballooning-like character, ie. it is localized to the outboard midplane, where the curvature is unfavorable. Such a mode could cause large radial transport near the outboard midplane of the plasma edge without significantly perturbing the transport away from the outboard edge, causing a collapse of the pedestals at the midplane. Once the collapse starts occurring at the midplane, the parallel gradients thus created will drive rapid parallel transport of plasma. Thus, one should expect to see an effect on the whole flux surface shortly after the onset of the mode, even if the mode is completely localized to the outboard midplane. Another possible explanation is that the mode starts near the x-point, which is at the bottom for these discharges. The effects of this mode would propagate along field lines into the view of the outboard edge array and then into the view of the top array. It may be possible to distinguish between the two possible explanations by studying the H-L transition in upper x-point plasmas, in which case the top array will be viewing the x-point region. If the mode originates at the x-point, then the collapse should be seen at the top first. If the mode originates at the outboard edge, the collapse should be seen at the outboard edge first. The parallel connection length between the outboard edge and the top of the plasma is roughly 1.5 m for the discharge presented here. If one assumes that the plasma disturbance travels along the field lines at a velocity near the ion acoustic velocity⁶ $\sqrt{(T_e + 3T_i)/m_D}$, and assumes $T_e = T_i = 200$ eV (characteristic of the pedestal region in H-mode), then the effects at the top of the plasma would be delayed 7 μ s, which is roughly in agreement with our observations. Future

measurements with a shorter response time of the amplification circuits should allow more accurate timing difference measurements.

VI. Summary

Two simultaneously operating soft x-ray arrays have been designed, installed, and operated on the Alcator C-Mod tokamak. The diagnostics provide simultaneous measurements of the radial profiles of soft x-ray emissivity at the top and the outboard edge with 1.2 and 1.5 mm resolution mapped to the outboard midplane. The soft x-ray emissivity profiles in both locations are pedestal-like in H-mode, but the pedestals have different positions, widths, and heights. This implies that the soft x-ray emissivity is not constant on the flux surfaces, as determined from the magnetic equilibrium reconstruction, violating the fundamental assumption in the inversion of the chord integrated measurements to local emissivity profiles. Thus, systematic errors in the inferred emissivity profiles are introduced. A numerical study of the magnitude of these systematic errors has been performed. We find that the absolute value of emissivity is generally overestimated at the outboard edge and underestimated at the top, but the total systematic error between the two measurements is on the order of $\leq 15\%$. The pedestal widths are reproduced with less than 15% error, and the pedestal locations remain accurate to within 1 mm. Therefore, the systematic errors introduced in the inversion are relatively benign. The system is capable of measuring timing differences on the order of $12 \mu\text{s}$, and this has been used to identify some H-L transitions which occur at the outboard edge before they are seen at the top of the plasma. This is consistent with a ballooning-like instability, or an instability originating at the x-point.

References

- ¹F. Wagner, G. Becker, K. Behringer, D. Campbell, A. Eberhagen, W. Engelhardt, G. Fussmann, O. Gehre, J. von Gernhardt, G. Gierke, G. Haas, M. Huang, F. Karger, M. Keilhacker, O. Klüber, M. Kornherr, K. Lackner, G. Lisitano, G.G. Lister, H.M. Mayer, D. Meisel, E.R. Müller, H. Murmann, H. Niedermeyer, W. Poschenrieder, H. Rapp, H. Röhr, F. Schneider, G. Siller, E. Speth, A. Stäbler, K.H. Steuer, G. Venus, O. Vollmer, Z. Yu, Phys. Rev. Lett. **49**, p. 1408 (1982)
- ²T. Sunn Pedersen, R.S. Granetz, A.E. Hubbard, I.H. Hutchinson, E.S. Marmor, J.E. Rice, J. Terry, “Radial Impurity Transport in the H-mode Transport Barrier Region in Alcator C-Mod”, submitted to Nucl. Fusion
- ³H. Zohm, Plasma Phys. Controlled Fusion **38** p. 1213 (1996)
- ⁴T. Sunn Pedersen and R.S. Granetz, Rev. Sci. Instrum. **70**, p. 586 (1999)
- ⁵M. Greenwald, R. Boivin, P. Bonoli, R. Budny, C. Fiore, J. Goetz, R. Granetz, A. Hubbard, I. Hutchinson, J. Irby, B. LaBombard, Y. Lin, B. Lipschultz, E. Marmor, A. Mazurenko, D. Mossessian, T. Sunn Pedersen, C.S. Pitcher, M. Porkolab, J. Rice, W. Rowan, J. Snipes, G. Schilling, Y. Takase, J. Terry, S. Wolfe, J. Weaver, B. Welch, S. Wukitch, Phys. Plasmas **6**, p. 1943 (1999)
- ⁶F. F. Chen, *Introduction to Plasma Physics and Controlled Fusion* vol. 1 (Plenum Press, New York, 1984) p. 96

Figure 1: This schematic shows the views of the two x-ray arrays in the Alcator C-Mod vessel. Flux contours for a typical plasma equilibrium are shown for comparison.

Figure 2: The soft x-ray emissivity profiles measured at the top and the outboard edge are both pedestal-like, but the pedestals are different with respect to their locations, widths, and heights. The slopes inside the pedestals are almost the same.

Figure 3: Contours of constant emissivity for a particular choice of two-dimensional emissivity function are shown in grey. The black contours show the flux surfaces as calculated by EFIT. The thickest contour indicates the separatrix. For each detector array, the lines of sight of the innermost and outermost detectors are also plotted.

Figure 4: The emissivity profiles from the two edge x-ray arrays shown here are obtained by assuming (erroneously) that the emissivity is constant on a flux surface. They are similar to emissivity profiles obtained from real experimental measurements.

Figure 5: This shows a comparison between the prescribed two-dimensional emissivity and the emissivity derived from the outboard midplane array, under the assumption of emissivity being constant on a flux surface. The emissivity is plotted as a function of R (major radius) for a fixed value of the Z (height above the vessel midplane) coordinate.

Figure 6: The prescribed emissivity, and that derived from the top array (array 2) under the assumption that the emissivity is constant on a flux surface, plotted as a function of Z at fixed major radius.

Figure 7: Four consecutive time samples, each separated by $20 \mu s$, show the emissivity profile at the outboard edge beginning to flatten before any change is seen at the top of the plasma.

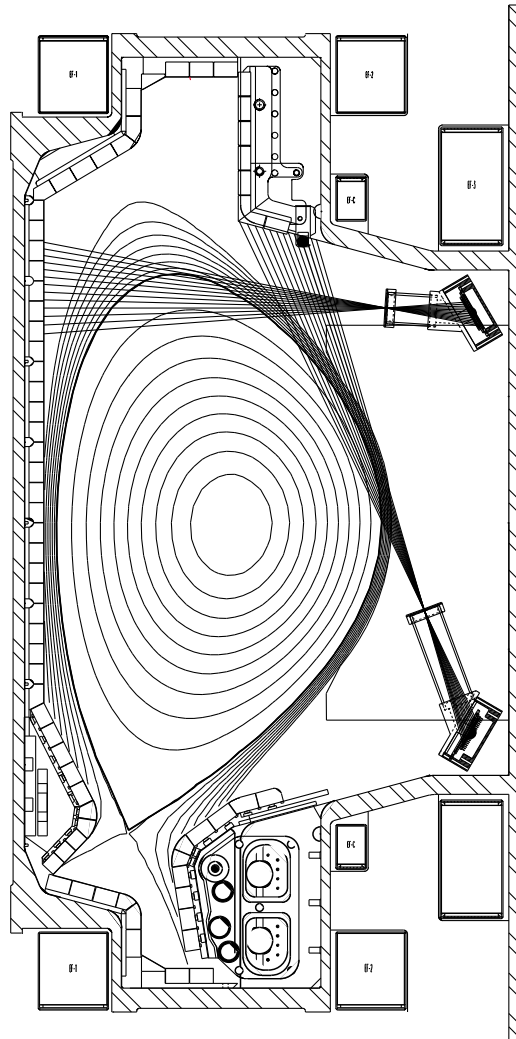


Figure 1:

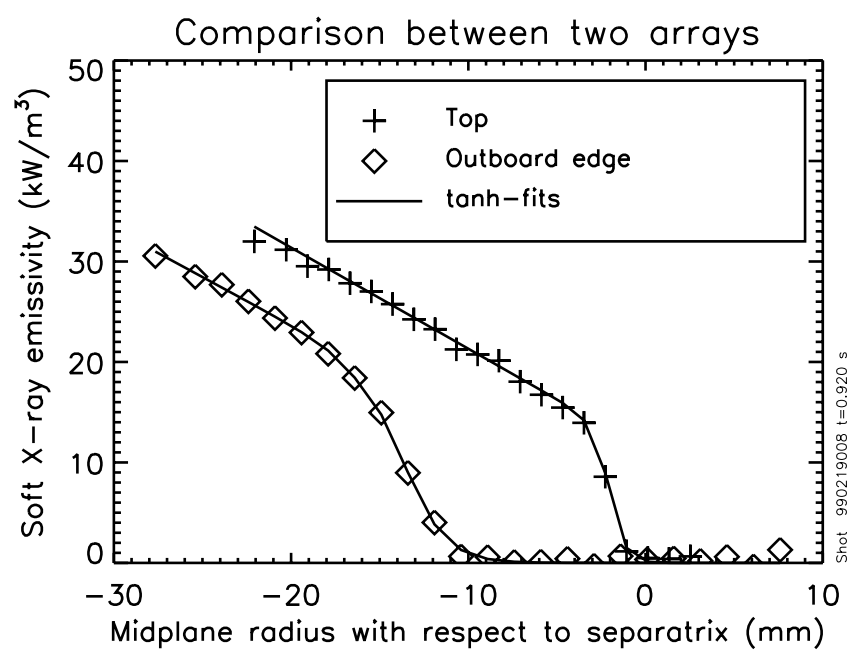


Figure 2:

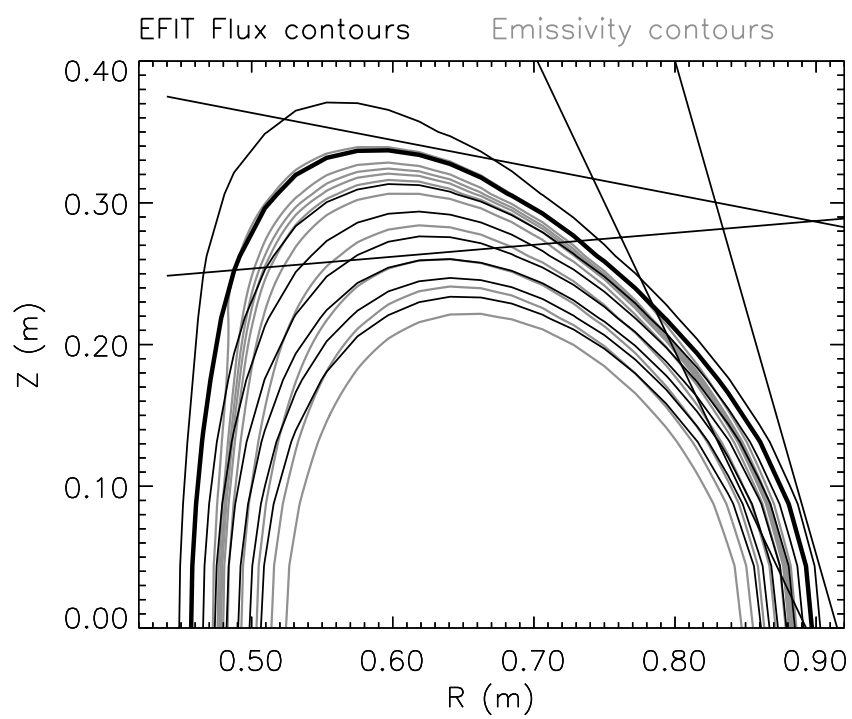


Figure 3:

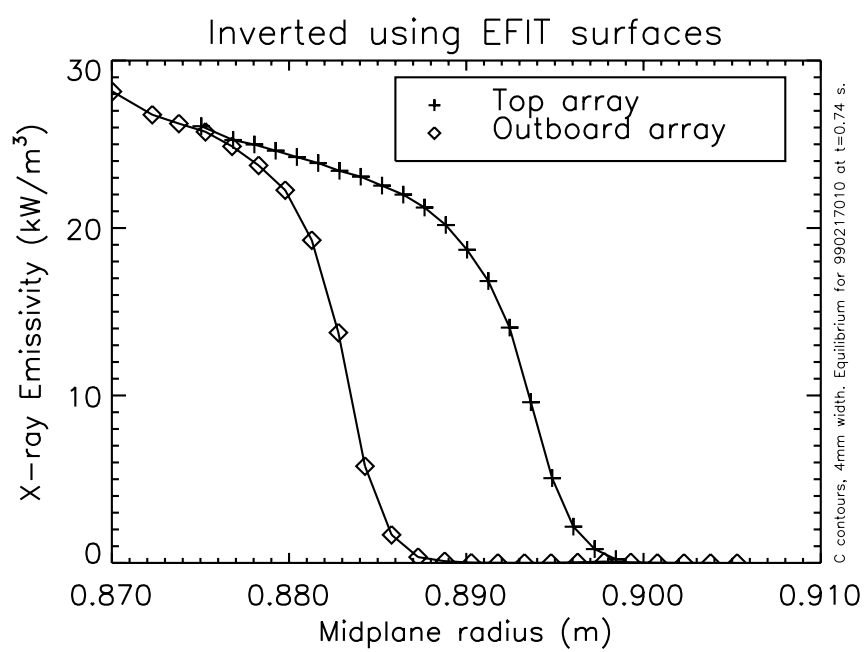


Figure 4:

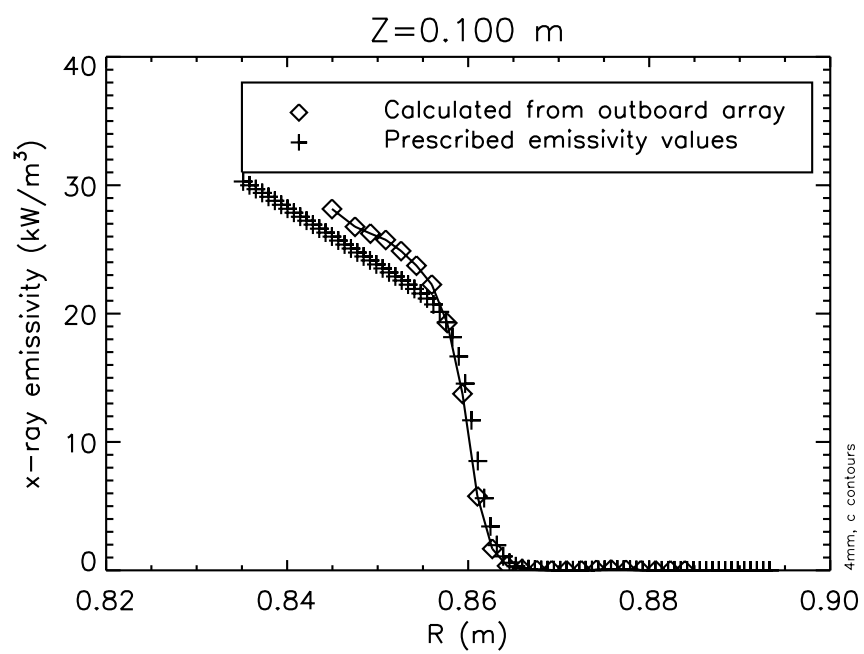


Figure 5:

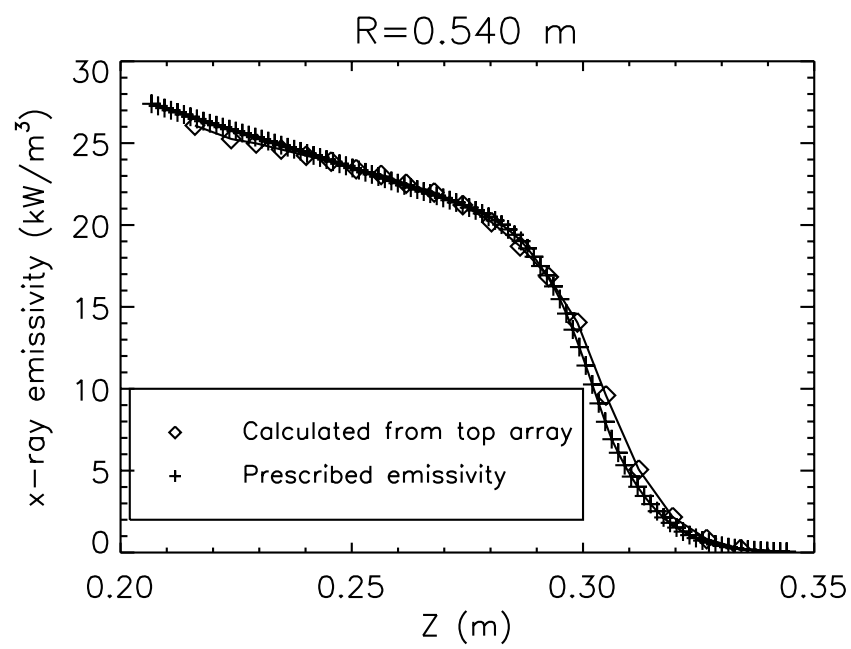


Figure 6:

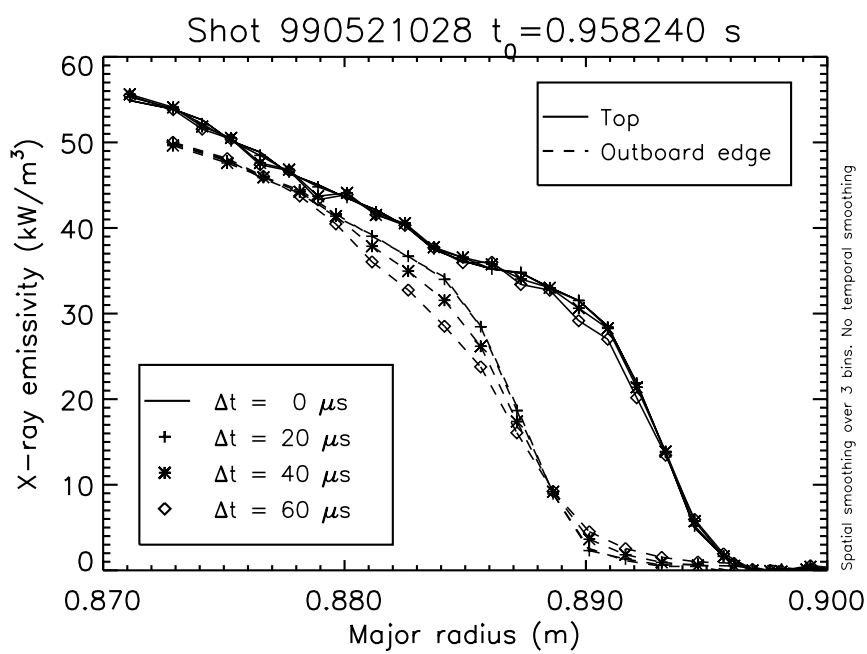


Figure 7: